Heat and Mass Transfer 37 (2001) 265–270 © Springer-Verlag 2001

Numerical study of the unsteady flow and heat transfer in channels with periodically mounted square bars

A. Valencia, J. S. Martin, R. Gormaz

Abstract Numerical investigations of unsteady laminar flow and heat transfer in a channel of height H with periodically mounted square bars of height $d = 0.2H$ arranged side by side to the approaching flow have been conducted for different transverse separation distances of the bars. Five cases with transverse separation distance of 0, 0.5, 1, 1.5 and $2d$ for a Reynolds number of 300 in a channel with a periodicity length of $2H$ were studied. The unsteady Navier–Stokes equations and the energy equation have been solved by a finite volume code with staggered grids combined with the SIMPLEC algorithm and a fine grid resolution. Due to the arrangement of bars detached from the channel walls the flow is unsteady with vortex shedding from the bars. The amplitude and mean values of the drag coefficients, skin friction coefficients, friction factor and Nusselt numbers have a strong dependence of the transverse separation distance of the bars.

List of symbols

C_{f1}	skin friction coefficient on the inferior wall, $\tau_w/(1/2\rho U_0^2)$
C_{f2}	skin friction coefficient on the superior wall, $\tau_w/(1/2\rho U_0^2)$
C_{d1}	drag coefficient on the inferior bar, $D/(1/2\rho U_0^2 d)$
C_{d2}	drag coefficient on the superior bar, $D/(1/2\rho U_0^2 d)$
d	bar height, m
D	drag, N m^{-1}
f	friction factor, $(H/2L)\Delta p/(1/2\rho U_0^2)$ also eddy shedding frequency, s^{-1}
G	transverse bar separation distance, m
h	heat transfer coefficient, W m^{-2} K^{-1}
H	channel height, m
k	thermal conductivity of air, W m^{-1} K^{-1}
L	periodicity length, m
Nu	averaged Nusselt number, hH/k
P	nondimensional pressure, $p/\rho U_0^2$
Pr	Prandtl number, ν/α
Re	channel Reynolds number, $U_0 H/\nu$
S	Strouhal number, fH/U_0
t	time, s
T	temperature, K
T_0	reference temperature, K
T_W	channel wall temperature, K
T_B	bulk temperature, K
u	Cartesian velocity component in the x direction, m s^{-1}
v	Cartesian velocity component in the y direction, m s^{-1}
U_0	channel-averaged velocity at the inlet, m s^{-1}
U	nondimensional Cartesian velocity component, u/U_0
V	nondimensional Cartesian velocity component, v/U_0
X	nondimensional Cartesian coordinate, x/H
Y	nondimensional Cartesian coordinate, y/H

Greek symbols

α	thermal diffusivity, m^2 s^{-1}
β	mean pressure gradient
θ	nondimensional temperature, T/T_0
ν	kinematic viscosity, m^2 s^{-1}
τ	nondimensional time, tU_0/H
τ_w	wall shear stress, N m^{-2}

1 Introduction

The technical backgrounds for this investigation are compact heat exchangers and cooling of electronic components. An analysis shows that their realization calls for the smallest hydraulic diameters, i.e., smallest Reynolds numbers, that can be realized. Often Reynolds number between 100 and 1000 are of interest, which implies a nominal laminar flow. Also the highest possible heat transfer coefficients, i.e., Nusselt numbers are a design aim. This heat transfer enhancement in laminar channel flows can be obtained by geometric modifications of the channel. These modifications induce vortices to augment transverse fluid mixing. Particular types of modifications allow to control generation and orientation of vortices. Principally transverse vortices and longitudinal vortices can be distinguished. Transverse vortices have their axes transverse to the flow and are consistent with two dimensional flow, while longitudinal vortices have their axes along the flow mainly in the streamwise direction and imply three dimensional flow.

Received on 28 January 2000

A. Valencia (✉)
Departamento de Ingeniería Mecánica
Universidad de Chile
Casilla 2777 Santiago Chile

J. S. Martin, R. Gormaz
Departamento de Ingeniería Matemática
Universidad de Chile
Casilla 170/3 Correo 3 Santiago Chile

The authors gratefully acknowledge the support of this work by the FONDAP-Chile.

For fully developed channel flows the investigations that have been made on the generation of vortices and their influence on flow structure and heat transfer, include longitudinal vortex generators in the form of winglets on the channel surface, and transverse vortex generators as cylinders, rectangular bars, baffles or grooved channels. An extensive coverage of the application of vortex generators for compact heat exchangers is given by Fiebig [1].

Although some additional space may be required to place vortex generators in the channel, the technique is passive, economical, and does not cause any undue vibrations or noise in the system. However, the beneficial effect of vortex generators is maximized only if they are optimally spaced in the channel in the longitudinal and transverse directions. This sensitivity of thermal performance to geometrical arrangement has spurred considerable interest in identifying optimal arrangements. For computation of laminar flow and heat transfer in channels with periodically mounted vortex generators periodic boundary conditions are imposed.

Valencia [2] studied the unsteady flow and heat transfer in plane channels with periodically mounted rectangular bars on the channel axis of height $0.5H$ and quantify the beneficial effects of self-sustained oscillations for three periodicity lengths of 2.25, 4.25 and $6.25H$. Calculations have been performed for Reynolds number from 100 to 400 ranging from steady laminar to lower transitional region. A comparison of mean Nusselt number as a function of the pumping power for the different configurations shows that for constant pumping power the Nusselt number decreases with the periodicity length.

Wang et al. [3] investigated the enhancement of heat transfer due to unsteady flow in channels with in-line and staggered ribs. For the in-line configuration, the flow becomes naturally unsteady at a critical Reynolds number around 110. For the staggered case, this value is around 200. Significant increases in heat transfer rate are reported once the flow becomes unsteady. To ascertain the validity of the periodic boundary condition for a computational domain of length L, they reported calculations made with a computational domain of length $3L$ for the staggered case. The temporal signals of the velocity and temperature at one point of the computational domain were in both cases similar.

The mechanism of heat transfer enhancement due to self-sustained oscillation in communicating channels was investigated by Amon et al. [4]. Flow instability generates a series of transverse vortices in the wake of the fins, leading to relative thin thermal boundary layers that further contribute to heat transfer augmentation on the fins. They observed self-sustained oscillation at a critical Reynolds number which was lower than the critical Reynolds number of the corresponding plane channel flow. In the low Reynolds number range the frequency values closely follow the three-wave Tollmien–Schlichting solution for plane channel flow.

Herman et al. [5] report experimental measurements of unsteady temperature distributions and local heat transfer in grooved and communicating channels. The Reynolds number in the communicating channels is defined as $\mathrm{Re}_c = 3Uh/2\nu$, where the characteristic length scale h in this definition represents the half-height of the main channel. The critical Reynolds number for the onset of oscillations was experimentally determinate to be around 200, the flow is time-periodic and exhibits a single fundamental frequency. In the regime of higher Reynolds number the flow is quasiperiodic and it mostly exhibits two dominant frequencies. By analyzing sequences of interferometric images, different oscillatory regimes and varying oscillatory regimes were detected. The authors notice the presence of four and three traveling waves over the double periodicity length of the channel. As the flow structure in the communicating region is in agreement with the traveling wave structure in the main channels, the vortical structures in two successive communicating regions are either identical or antisymmetric respectively.

Dejong et al. [6] compared experimental and numerical results for flow and heat transfer in similar offset strip-fin geometries. The flow is observed to follow a sequence of transitions. At very low Reynolds number the flow is steady and above a critical Reynolds number the flow becomes unsteady with a single dominant frequency. At even higher Reynolds numbers an additional lower frequency is generated and with subsequent increase in Re the flow becomes turbulent. The unsteady regime is marked by transverse vortices that are generated at the leading edges of the fin element, which travel down on the top and bottom surfaces of the fin element. These transverse vortices play a key role in significantly enhancing the local heat transfer by bringing fresh fluid from the freestream towards the fin surface.

Kapat et al. [7] report on laminar-to-turbulent transition in a rectangular channel in the presence of periodically placed cylindrical eddy promoters. Placement of the eddy promoters in the channel, depending on the geometric configuration, can significantly reduce the value of Reynolds number at transition. The critical Reynolds number decreases, by more than a factor of three, from 1500 for plane channel to about 400 for the most unstable deployed configuration.

Karniadakis et al. [8] show that the addition of small cylinders in a plane channel results in stability modes that are little changed in form or frequency from plane-channel Tollmien–Schlichting waves. However, for eddy-promoter flow in which the cylinder is placed near the center of the channel, the instability-mode spatial structures are consistent with the Karman vortex street. In this case the vorticity generation at the channel-walls next to the cylinders and on the cylinder surface is the most important fraction of the total vorticity generation in the system.

In spite of these recent efforts, the effects of the transverse separation distance of periodically mounted bars in a laminar channel flow on heat transfer have not been reported in the literature. Therefore this work was undertaken to provide information on the unsteady flow and heat transfer processes in channels with periodically mounted square bars and to quantify the beneficial effects of self-sustained oscillations. Calculations have been performed for several transverse bar separation distances for a nominal laminar Reynolds number of 300.

2 Mathematical formulation

The flow and temperature fields are governed by the continuity, nonsteady two dimensional Navier–Stokes and energy equation. The fluid properties are assumed to be constant and the dissipation terms in the energy equation are neglected.

$$\frac{\partial U}{\partial X}+\frac{\partial V}{\partial Y}=0 \tag{1}$$

$$\frac{\partial U}{\partial \tau}+\frac{\partial U^2}{\partial X}+\frac{\partial UV}{\partial Y}=-\frac{\partial P'}{\partial X}+\beta+\frac{1}{\mathrm{Re}}\left(\frac{\partial^2 U}{\partial X^2}+\frac{\partial^2 U}{\partial Y^2}\right) \tag{2}$$

$$\frac{\partial V}{\partial \tau}+\frac{\partial UV}{\partial X}+\frac{\partial V^2}{\partial Y}=-\frac{\partial P'}{\partial Y}+\frac{1}{\mathrm{Re}}\left(\frac{\partial^2 V}{\partial X^2}+\frac{\partial^2 V}{\partial Y^2}\right) \tag{3}$$

$$\frac{\partial \theta}{\partial \tau}+\frac{\partial U\theta}{\partial X}+\frac{\partial V\theta}{\partial Y}=\frac{1}{\mathrm{RePr}}\left(\frac{\partial^2 \theta}{\partial X^2}+\frac{\partial^2 \theta}{\partial Y^2}\right) \tag{4}$$

The velocity components have been nondimensionalised with the average velocity U_0 and the length with the channel height H. Re is the Reynolds number and Pr is the Prandtl number. The present numerical solutions will assume periodicity of the solution over one basic unit and therefore the actual computational geometry will be limited to this basic unit. Implicit in this treatment is the assumption that the flow is fully developed, both hydrodynamically and thermally.

To enable periodic boundary conditions, the instantaneous nondimensional pressure P is decomposed into a mean part β that is assumed to vary linearly in X, and a fluctuating part P' that vary in X and Y, Pantankar et al. [9]. Thus:

$$P(X,Y,\tau)=-\beta(\tau)X+P'(X,Y,\tau) \tag{5}$$

This mean gradient β is adjusted every time step to satisfy the fixed mass flow condition. Boundary conditions are imposed on intermediate velocities and on the fluctuating part of the pressure.

The thermal boundary conditions are uniform channel walls temperature T_W and the bars do not have imposed temperature. The redevelopment of the thermal boundary layer on interrupted surfaces has a significant impact on heat transfer enhancement, if the heating is applied to the vortex generators. The bars here only generate transverse vortices and the heat transfer surface is the same as in a plane channel without mounted bars. For the periodic thermally developed domain, the temperature difference:

$$\frac{T(0,y,t)-T_W}{T_B(0)-T_W}=\frac{T(L,y,t)-T_W}{T_B(L,t)-T_W} \tag{6}$$

can be considered to be periodic along the x direction. The periodicity condition (6) enables the solution domain for the temperature problem limited to the streamwise length L. This periodic thermally developed regime is a logical generalization of the conventional thermally developed regime, Pantankar et al. [9].

The bulk temperature was calculated using the velocity and the temperature distribution with the equation:

$$T_B(x,t)=\frac{\int_0^H |u|T\,dy}{\int_0^H |u|\,dy} \tag{7}$$

Instantaneous local heat transfer will be expressed in terms of the local Nusselt number based on channel height and can be written as:

$$\mathrm{Nu}_x=\frac{h_x H}{k}=\frac{(\partial T/\partial y)_{\mathrm{wall}} H}{(T_B(x,t)-T_W)} \tag{8}$$

The flow losses are evaluated with the friction factor defined as:

$$f=\beta=1/2(C_{f1}+C_{f2})+C_{d1}\frac{d}{2L}+C_{d2}\frac{d}{2L} \tag{9}$$

where C_{f1} and C_{f2} are the skin friction coefficients on the channel walls, and C_{d1} and C_{d2} are the drag coefficients of the inferior and superior bars mounted in the channel.

3 Computational details

The fully developed air flow through the channel geometry with periodically mounted square bars as vortex generators can be numerically modeling through a basic unit containing a single pair of bars. Figure 1 schematically shows the computational domain. The streamwise periodicity length of the domain is $L = 2H$ and two bars of height $0.2H$ are mounted detached from the channel walls. The computations were made for five transverse bar separation distances $G = 0$, 0.5, 1, 1.5, and $2d$ for a Reynolds number of 300. For this Reynolds number and a periodicity length $L = 2.25H$ the flow in a channel with a mounted rectangular bar on the channel axis of height $0.5H$ and wide of $0.25H$ is unsteady and laminar, Valencia [2].

The discretization method used in the present study uses a control volume formulation. A detailed description of this discretization method is given by Patankar [10]. Several modifications to the application of SIMPLE method were recommended by van Doormaal and Raithby [11], including the SIMPLEC approximation, tridiagonal-matrix solver and convergence criterion for the pressure correction equation. These modifications are employed in the present algorithm. For the solution of the resulting matrices with periodic boundary conditions a special tridiagonal-matrix solver was programed. On the rectangular

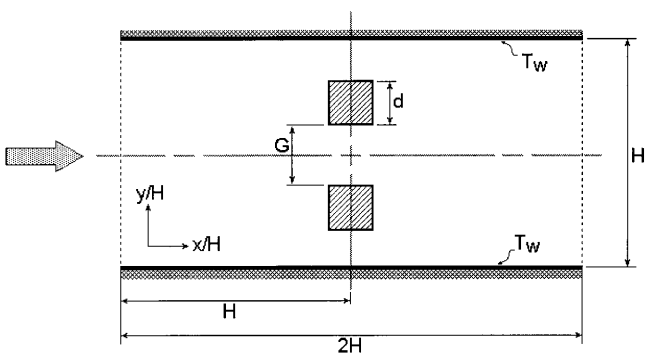

Fig. 1. Computational domain

bars, the same governing equations are used. A zero velocity field on the bars are achieved by adding a source term of very high magnitude in the Navier–Stokes equations in the control volumes where the bars are located.

For the computations a fine grid with 162×82 control volumes and time spacing of 0.001 has been used. The time step satisfied the Courant–Friedrich–Levi condition, and approximately 1000 time steps are needed for one time period, and a typical run of 30000 time steps of size equal to 0.001 units of time takes about 6000 CPU minutes on an Pentium III computer.

In order to simulate this flow produced in the channel with a sequence of identical pairs of square bars, it is usual to simplify the problem considering a periodic one, each period containing one pair. This simplification assumes that the spatial period of the solution is equal to the geometrical period of the domain. We have carried out numerical simulations of the periodic problem with a period length containing n pairs of mounted square bars for $n = 1, 2, 3, 4$ with $G = 0d$ to prove this hypothesis in this case. In order to reduce the discretization error we need to use the same fine grid of 162×82 nodes per periodicity length. To carried out these simulations with $n > 1$ we have used a Silicon Graphics workstation with 6 processors and we have paralleled the numerical code. The flow structure in two successive periodic regions was symmetric, and the computed differences on the global Nusselt number, drag coefficients, mean skin friction coefficients, and Strouhal number between the one, two, three or four period cases were small of 1%.

To check grid independence, numerical simulations of the unsteady problem with $G = 0d$ were performed on grids of 82×42, 130×66 and 162×82 control volumes. Values of integral parameters as the mean drag coefficients, mean skin friction coefficients, mean Nusselt number on the channel walls, friction factor, and eddy-shedding Strouhal number of the flow were compared. The differences on these parameters between the two more finer grids were inferior to 2%. In spite of this results with the middle grid, the finest grid will be used for all calculations in this paper for the correct simulation of these unsteady laminar flows.

4
Results and discussion

The structure of the flow in the periodic region will be now discussed. It will be illustrated through the use of computed instantaneous velocity vectors. Figure 2 shows instantaneous maps of fluctuating velocity vectors for the five arrangements with different transverse bar separation distances $G/d = 0$, 0.5, 1, 1.5, and 2, for a Reynolds number of Re = 300. One can notice vortices generated in the channel downstream the bars, and in the cases with $G/d = 0$, 1.5, and 2 also vortices upstream the square bars, these vortices exchange the core fluid with the near-wall

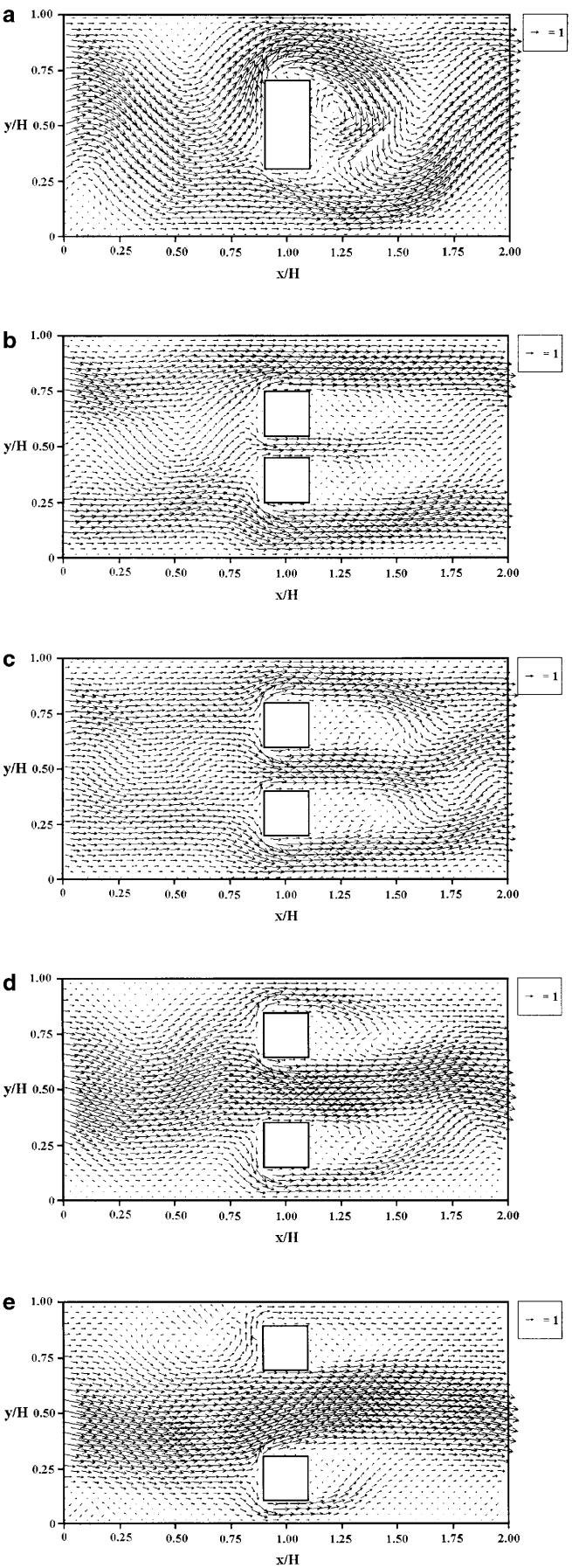

Fig. 2. Instantaneous maps of velocity vectors for the five cases with Re = 300: **a** $G/d = 0$, **b** $G/d = 0.5$, **c** $G/d = 1$, **d** $G/d = 1.5$, and **e** $G/d = 2$

fluid. The Karman vortex sheets are alternately shed by the downstream face of the bars and these travel diagonally through the channel, washing across the upstream face of the next bars. Thus, the upstream face of the bars are exposed to a flushing condition induced by the periodic boundary condition. The Fig. 2b and c show that the flow pattern are similar for the transverse bar separation distances $G/d = 0.5$ and 1. For transverse bar separation distances $G/d = 1.5$ and 2, Fig. 2d and e, the flow pattern show vortices upstream the bars, due the fluid acceleration between the bars. In the case with $G/d = 2$ a big vortex can be observed upstream the superior bar, Fig. 2e. In this configuration a complex interaction exists among the presence of the channel walls and the transverse separation distance between the bars in the generation of the unsteady vortices. Therefore two flow pattern can be distinguished, for $G > 1$ the flow accelerates in the gap between the bars, and induces vortices upstream the bars, for $G \leq 1$ the flow accelerates in the gap between the bars and the channel walls.

Figure 3 shows the time averaged local skin friction coefficient on the inferior channel wall for different transverse bar separation distances. The local skin friction factor takes a maximum at the inserted position of the bars. The skin friction on the wall decreases with G/d upstream and downstream the bars. In the inlet and exit of the computational domain the values are in all the cases the same, due the imposed periodic boundary conditions.

Figure 4 shows the influence of the unsteady vortices on time averaged local Nusselt numbers at the inferior

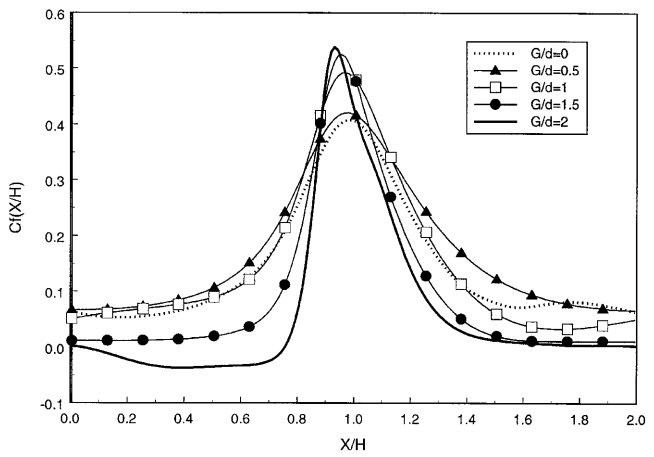

Fig. 3. Time averaged local skin friction coefficient on the inferior wall for the five cases

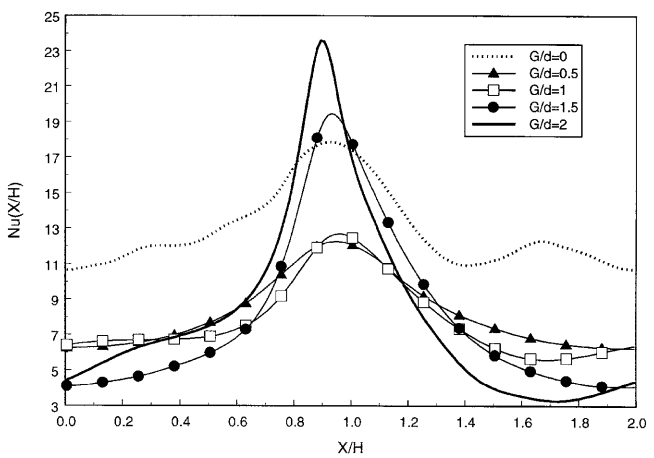

Fig. 4. Time averaged local Nusselt number on the inferior wall for the five cases

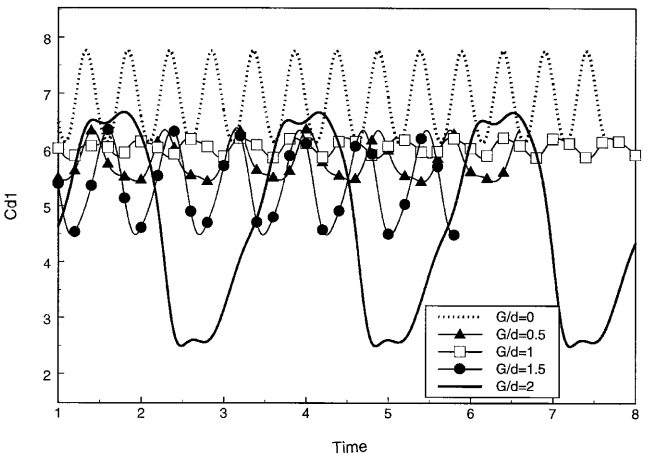

Fig. 5. Mean drag coefficient on the inferior bar for the five cases as function of nondimensional time

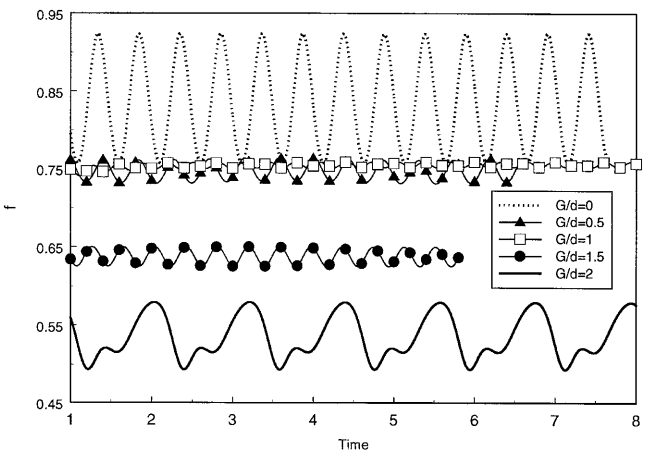

Fig. 6. Friction factor for the five cases as function of nondimensional time

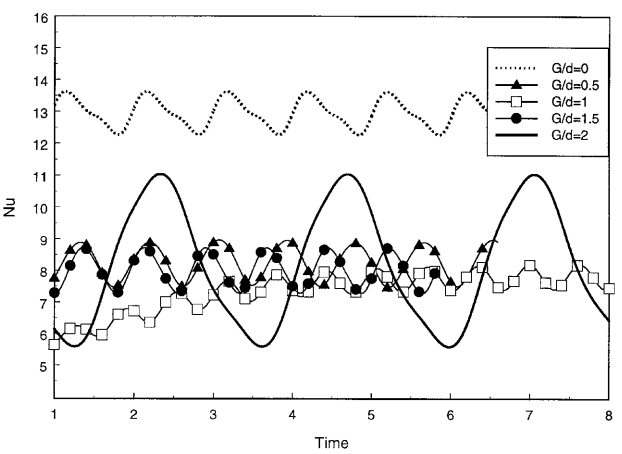

Fig. 7. Nusselt number for the five cases as function of nondimensional time

Table 1. Mean values of Strouhal number, skin friction, drag, friction factor, Nusselt number and performance evaluation for different transverse bar separation distances

G/d	S	C_f	C_{d1}	f	Nu	$Nu/Nu_0/(f/f_0)^{1/3}$
0	0.987	0.146	6.92	0.838	12.97	1.25
0.5	1.157	0.169	5.78	0.748	8.25	0.82
1	1.558	0.150	6.02	0.752	7.13	0.71
1.5	0.647	0.100	5.39	0.638	7.98	0.84
2	0.423	0.066	4.56	0.535	8.21	0.92

channel wall for the five transverse bar separation distances. The form of local heat transfer on the wall for $G/d = 0$ is different to the arrangements with $G > 0$, the effects of the vortices are more expanded in the channel in this case, Fig. 2a. The form of the local Nusselt numbers with $G/d = 0.5$ and 1 are similar. For transverse bar separation distances $G/d = 1.5$ and 2 the maxima of Nusselt numbers are bigger than with $G/d = 0$, due the small distance of the bar to the channel wall in these cases.

Figure 5 shows the influence of vortex sheets that are alternately shed by the inferior bar on computed instantaneous drag coefficient for the five studied arrangements. The instantaneous drag coefficients are periodic, however the mean value, amplitude and frequency are strong dependent of G/d. For the case with $G/d = 2$ the bigger temporal variations of drag are observed, and the period of vortex shedding is also bigger as in the other cases. The interactions that exist among the channel walls, the mounted bars, and the periodic boundary conditions in the generation of the unsteady vortices cause the big variations of the drag coefficients.

The effects of the vortex shedding on the temporal variation of mean pressure drop in the channel represented by the friction factor f, are shown in Fig. 6. The case with $G/d = 0$ has the biggest mean values and amplitudes of f. The cases with $G/d = 0.5$ and 1 are similar, and for the case with $G/d = 2$, one can notices that the form of f is different, as consequence of the temporal variation of drag coefficients on the bars, Fig. 5.

The mean heat transfer coefficient or Nusselt number on the channel walls also varies with the time, Fig. 7 shows the variations of Nusselt number on the inferior wall of the channel. The form of the variation of Nu for the cases $G/d = 0.5$, 1 and 1.5 are similar. The biggest temporal variations are observed for the case with $G/d = 2$. The mean value for the case with $G/d = 0$ it is much bigger that in the cases with $G/d > 0$. These results indicate that the fluid flow between the mounted square bars has a negative effect on heat transfer.

Table 1 shows the mean values of Strouhal number, skin friction, drag, friction factor, Nusselt number and performance evaluation for the five studied arrangements. Nu_0 and f_0 are the Nusselt number and friction factor in a channel without mounted vortex generators, ($Nu_0 = 3.77$, $f_0 = 12/Re$). The frequency of the vortex shedding or Strouhal number S decreases strongly for $G/d > 1$. Table 1 shows that the arrangements with $G/d = 0.5$ and 1 have similar values of drag coefficients and friction factor, but the heat transfer coefficients are not similar. In comparing the performance of the channel with the mounted square bars and plane channels, it is necessary to specify the constraints under which comparison is made. In this work, the comparison of heat transfer enhancement is made for the constraint of constant pumping power. Table 1 shows the augmented heat transfer per unit pumping power for the five studied cases, the best performance has the arrangement with $G/d = 0$, followed by the arrangement with $G/d = 2$.

5 Conclusion

In this paper, we have employed numerical simulations to explore the fluid flow and heat transfer in channels with periodically mounted square bars. The effects of unsteady vortex shedding have been captured by solving the Navier–Stokes and energy equations in two-dimensions. Computations were made for five transverse bar separation distances, $G/d = 0$, 0.5, 1, 1.5, and 2 for a constant Reynolds number and periodicity length. The numerical results reveal the complex structure of the unsteady flow. As a consequence of the self-sustained oscillations, there is a important heat transfer enhancement on the channel walls. The interaction of fluid flow between the bars and the fluid flow between the bars and the channel walls affects considerably the performance of these configurations.

References

1. **Fiebig M** (1997) Vortices and heat transfer. ZAMM. Zeitschrift für Angewandte Mathematik and Mechanik 77: 3–18
2. **Valencia A** (1999) Heat transfer enhancement due to self-sustained oscillating transverse vortices in channels with periodically mounted rectangular bars. Int J Heat and Mass Transfer 42: 2053–2062
3. **Wang G; Stone K; Vanka SP** (1996) Unsteady heat transfer in baffled channels. J Heat Transfer 118: 585–591
4. **Amon CH; Majumdar D; Herman CV; Mayinger F; Mikic BB; Sekulic DP** (1992) Numerical and experimental studies of self-sustained oscillatory flows in communicating channels. Int J Heat and Mass Transfer 35: 3115–3129
5. **Herman C; Kang E; Wetzel M** (1998) Expanding the applications of holographic interferometry to the quantitative visualization of oscillatory thermofluid processes using temperature as tracer. Exp Fluids 24: 431–446
6. **Dejong NC; Zhang LW; Jacobi AM; Balachandar S; Tafti DK** (1998) A complementary experimental and numerical study of the flow and heat transfer in offset strip-fin heat exchangers. J Heat Transfer 120: 690–698
7. **Kapat JS; Ratnathicam J; Mikic BB** (1994) Experimental determination of transition to turbulence in a rectangular channel with eddy promoters. J Fluids Eng 116: 484–487
8. **Karniadakis G; Mikic BB; Patera AT** (1988) Minimum-dissipation transport enhancement by flow destabilization: Reynolds' analogy revisited. J Fluid Mech 192: 365–391
9. **Patankar SV; Liu CH; Sparrow EM** (1977) Fully developed flow and heat transfer in ducts having streamwise-periodic variations of cross-sectional area. J Heat Transfer 99: 180–186
10. **Patankar SV** (1980) Numerical Heat Transfer and Fluid Flow. Hemisphere, Washington, DC
11. **Doormaal JP van; Raithby GD** (1984) Enhancements of the SIMPLE method for predicting incompressible fluid flows. Numerical Heat Transfer 7: 147–163